

Crystal growth and characterization of the model high-temperature superconductor  $\text{HgBa}_2\text{CuO}_{4+\delta}$

Xudong Zhao,<sup>1,2</sup> Guichuan Yu,<sup>3</sup> Yong-Chan Cho,<sup>1</sup> Guillaume Chabot-Couture,<sup>4</sup> Neven Barišić,<sup>1</sup> Philippe Bourges,<sup>5</sup> Nobuhisa Kaneko,<sup>1</sup> Yuan Li,<sup>3</sup> Li Lu,<sup>4</sup> Eugene M. Motoyama,<sup>3</sup> Owen P. Vajk,<sup>6</sup> and Martin Greven<sup>1,4,\*</sup>

<sup>1</sup>Stanford Synchrotron Radiation Laboratory, Stanford, California 94309, USA

<sup>2</sup>Department of Physics, Jilin University, Changchun 130023, Peoples Republic of China

<sup>3</sup>Department of Physics, Stanford University, Stanford, California 94305, USA

<sup>4</sup>Department of Applied Physics, Stanford University, Stanford, California 94305, USA

<sup>5</sup>Laboratoire Léon Brillouin, CEA-CNRS Saclay, 91191 Gif-sur-Yvette Cedex, France

<sup>6</sup>NIST Center for Neutron Research, National Institute of Standards and Technology, Gaithersburg, Maryland 20899, USA

[\*] e-mail: [greven@stanford.edu](mailto:greven@stanford.edu)

[\*\*] The authors would like to acknowledge discussions with H. Eisaki and T.H. Geballe.

This work was supported by the DOE under Contract No. DE-AC02-76SF00515 and by the NSF under Grant No. 0405655.

Since the discovery of high- $T_c$  superconductivity in  $\text{La}_{2-x}\text{Ba}_x\text{CuO}_4$  in 1986,<sup>[1]</sup> the study of the lamellar copper oxides has remained at the forefront of condensed matter physics. Apart from the unusually high values of  $T_c$ , these materials also exhibit a variety of complex phenomena and phases. This rich behavior is a consequence of the lamellar crystal structures, formed of copper-oxygen sheets separated by charge reservoir layers, and of the strong electron-electron correlations in the copper-oxygen sheets. After two decades of intensive research, which has stimulated many valuable new insights into correlated-electron systems in general, there remains a lack of consensus regarding the correct theory for high- $T_c$  superconductivity. The ultimate technological goal of room-temperature superconductivity might only be attained after the development of a deeper understanding of the mercury-based compounds  $\text{HgBa}_2\text{Ca}_{n-1}\text{Cu}_n\text{O}_{2n+2+\delta}$ , the materials with the currently highest values of  $T_c$ .

One very important issue in this regard is the role of electronic vs. chemical and structural inhomogeneities in these materials, and the associated need to separate materials-specific properties from those that are essential to superconductivity.<sup>[2-5]</sup> Unfortunately, there has been remarkably little scientific work on the mercury-based compounds, since sizable crystals have not been available; quantitative measurements of any kind can be expected to become invaluable benchmarks for tests of theories of high- $T_c$  superconductivity.

The compounds  $\text{HgBa}_2\text{Ca}_{n-1}\text{Cu}_n\text{O}_{2n+2+\delta}$  can be viewed as model systems not only because of their record values of  $T_c$ , but also due their high-symmetry tetragonal crystal structures. Of particular interest is the simplest member of this materials family,  $\text{HgBa}_2\text{CuO}_{4+\delta}$  (Hg1201), which possesses only one copper-oxygen sheet in the unit cell

( $n=1$ ), as shown schematically in Fig. 1a. The largest crystals obtained by previous growth methods do not exceed  $1 \text{ mm}^3$ , and hence are insufficient in size for detailed studies by many experimental techniques. Here we report a novel recipe for the growth of Hg1201 crystals as well as detailed sample characterization results, including initial inelastic magnetic neutron scattering data. We note that samples grown by the method described here already have enabled recent optical conductivity,<sup>[6]</sup> inelastic x-ray scattering,<sup>[7]</sup> and angle-resolved photoemission<sup>[8]</sup> studies.

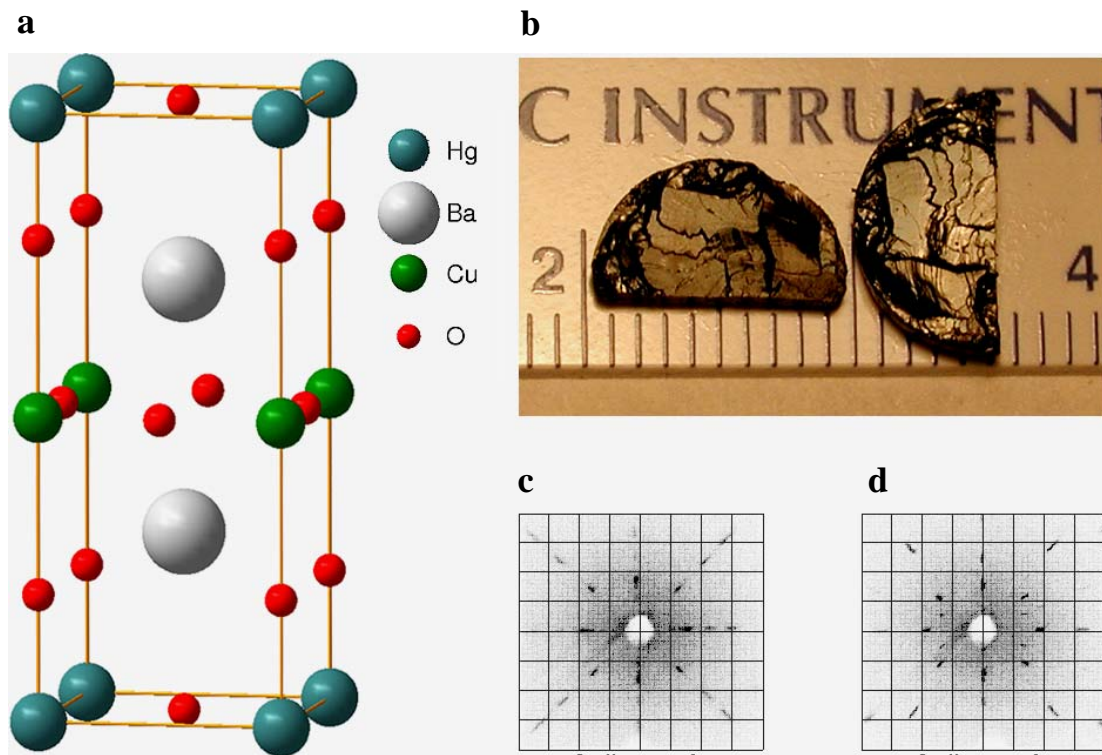


Figure 1. Large Hg1201 single crystal with unit cell and Laue pictures. a) Schematic of the tetragonal Hg1201 crystal structure. b) Photograph of a large Hg1201 crystal that was cleaved into two pieces of about equal size. The two pieces have a total

mass of nearly 1 g, corresponding to a volume of approximately 100 mm<sup>3</sup>. c) a-b plane and d) a-c plane Laue patterns.

One of the major difficulties in growing Hg<sub>1201</sub> crystals is the high vapor pressure of mercury oxide during the crystal growth, which requires growth via encapsulation or high-pressure techniques. In addition, sample preparation must be handled with special care, since mercury is highly toxic. The various growth techniques are summarized in Table 1. The high-static-pressure synthesis technique (belt-type high-pressure apparatus) is very effective, not only for Hg<sub>1201</sub>, but also for the four- and five-layer ( $n = 4, 5$ ) compounds.<sup>[9]</sup> However, this technique is not well-suited for the growth of single crystals. A relatively new technique, based on the application of high Ar gas pressure up to 11 kbar, allows the growth of single crystals.<sup>[10]</sup> However, due to the small chamber size of the high-pressure apparatus (several cm<sup>3</sup>), the crystal size is limited. Conventional encapsulation methods also allow crystal growth.<sup>[11-19]</sup> Based on this scheme, several improvements were developed, including the use of a three-zone furnace to control the mercury partial pressure; all these efforts resulted in either powder samples or sub-mm<sup>3</sup> sized crystals.<sup>[18,20-23]</sup> In contrast with the sophisticated methods mentioned above, we adopted a conventional encapsulation approach. The problems associated with high vapor pressure were solved by using thick-wall high-quality quartz tubes, by carefully dosing and mixing of HgO with the precursor, and by finding an adequate temperature profile for the crystal growth, thus allowing the tuning of the kinetics of the chemical reactions.

Synthesis of high-quality precursor material is a very sensitive step in the crystal growth. It is essential to produce a very clean precursor containing only barium, copper and oxygen, with the correct stoichiometry of 2:1:3. Impurities tend to prevent proper chemical reaction, and thus influence the crystal growth. Therefore, any contamination should be eliminated, if possible. The different methods of precursor preparation are also summarized in Table 1. A straightforward method is to simply mix BaO or BaO<sub>2</sub> with CuO.<sup>[11,12]</sup> Unfortunately, at room temperature, barium oxide or peroxide easily reacts with water or CO<sub>2</sub>, forming Ba(OH)<sub>2</sub> or BaCO<sub>3</sub>. For this reason, the commercially available BaO is contaminated, and consequently not suitable for precursor preparation. Both types of contamination negatively affect the crystal growth: Ba(OH)<sub>2</sub> releases water during the synthesis, which increases the pressure and may cause an explosion of the sealed quartz tube, and BaCO<sub>3</sub> can act as an impurity, perturbing the crystal growth.<sup>[9]</sup> An alternative precursor preparation method involves heating a mixture of BaCO<sub>3</sub> and CuO to temperatures exceeding 1100 °C.<sup>[15,16]</sup> A problem with this approach arises from the slow decomposition of the BaCO<sub>3</sub>, even at high temperature, and this method is therefore unpractical. In order to improve the homogeneity of the precursor, a third approach, the sol-gel method, was employed by several groups.<sup>[17,18,24]</sup> However, the use of organic acid or polymer can easily contaminate the precursor with carbon. A fourth method uses a mixture of Ba(NO<sub>3</sub>)<sub>2</sub> and CuO.<sup>[13,14]</sup> Further improvement of this method involves reacting BaCO<sub>3</sub> with HNO<sub>3</sub> and drying the resulting aqueous solution by freeze- or spray-drying to synthesize a homogeneous precursor.<sup>[19]</sup> We used this fourth method of precursor preparation, but found that the latter step is unnecessary and that commercially available Ba(NO<sub>3</sub>)<sub>2</sub> is sufficient.

Table 1. Techniques for the preparation of Hg1201 and of precursor materials

Techniques for Hg1201 preparation	Methods of precursor preparation	Product	Reference
Encapsulation	Mixture of oxides or peroxides	Powder	11, 12
Encapsulation	Mixture of nitrates	Powder in Ref. 13; crystal size $0.5 \times 0.5 \times 0.3 \text{ mm}^3$ in Ref. 14	13, 14
Encapsulation	Mixture of carbonates and CuO	Powder in Ref. 15; crystal size $3 \times 2 \times 0.1 \text{ mm}^3$ in Ref. 16	15, 16
Encapsulation	Sol-gel method with citrates and tartrates	Powder	17
Encapsulation; $\text{Mn}_2\text{O}_3/\text{Mn}_3\text{O}_4$ couple for oxygen partial pressure control	Sol-gel method with citrates	Powder	18
Encapsulation	Drying of aqueous nitrate solution	Powder	19
Three zone Encapsulation with Hg and oxygen modulation	Sol-gel by polymerization	Powder	24
High static pressure	Sol-gel by polymerization	Powder	9
High gas pressure	Mixture of $\text{BaCuO}_2\text{-CuO}$	Crystal size $0.4 \times 0.4 \times 0.02 \text{ mm}^3$	10
Encapsulation	Stoichiometric, contamination-free mixture of nitrates	Crystal size exceeding $100 \text{ mm}^3$	Present work

We emphasize the importance of the calcination procedure. To avoid the gas back-flow commonly found in conventional tube furnaces, we designed a special precursor preparation system that employed a quartz kettle and continuous oxygen flow. After mixing and grinding of  $\text{Ba}(\text{NO}_3)_2$  and CuO, the prepared powder was put into the kettle and heated up to  $920 \text{ }^\circ\text{C}$ . This method enabled us to obtain high-quality precursor material for the crystal growth.

For the reasons mentioned above, fresh precursor powder (which contains BaO) should be immediately mixed with mercury oxide, placed in a crucible, and sealed in the quartz encapsulation tube under vacuum. We used quartz tubes with dimensions 15 mm (inner diameter), 2.5 mm (thickness), and 100 mm (height), and crucibles with typical dimensions of 10 mm (inner diameter) and 80 mm (height). Particular attention was devoted to the choice of crucible material. Crucibles containing silica are unusable, due to the reaction between the silica and copper oxide. We also tried alumina crucibles, but found that, at elevated temperatures, CuO creeps up the crucible wall and eventually reacts with the quartz tube. This tendency also changes the composition of the material in the crucible. Furthermore, crystals tend to be contaminated with Al and to stick to the crucible walls, and hence are difficult to extract. We established that zirconia crucibles contain the CuO solution during the crystal growth and have the best overall characteristics.

The precursor (mass 2.14 g) and HgO (1.20 g) were mixed with stoichiometric proportions. In addition, about 0.3 g of excess HgO was added in order to compensate for the vaporized Hg and to obtain sufficiently high vapor pressure. By fine-tuning the amount of excess HgO, we were able to optimize growth conditions and to avoid explosion of the sealed quartz tube. The sealed quartz tube was placed in a conventional box furnace and heated up to 800 °C. At this temperature, solid-state reaction begins and the Hg1201 phase is formed. We benefited from this reaction, as it lowers the HgO pressure in the encapsulation tube, by keeping the furnace at this temperature for 10 hours. Then, the temperature was gradually increased to 1020 °C, which melted the

contents of the crucible and lead to a homogeneous pre-crystallization admixture. We found that slow-cooling at the rate of 2°C/h ensured equilibrium crystallization.

Figure 1b shows a picture of two halves of an as-grown Hg1201 crystal, which was cut out of the crucible using a wire saw and subsequently cleaved parallel to the *a-b* planes. Its orientation was determined from the Laue patterns shown in Fig. 1c and Fig. 1d. The four-fold pattern in Fig. 1c is consistent with the known tetragonal crystal symmetry (space group *P4/mmm*). XRD characterization of smaller samples demonstrated that our crystals are typically single-phase. The extracted room-temperature lattice parameters for as-grown crystals are  $a = 3.886 \text{ \AA}$  and  $c = 9.517 \text{ \AA}$ , in agreement with previously published results.<sup>[11,12,14]</sup>

A known feature of Hg1201 is the Hg off-stoichiometry, with a Hg deficiency that has been found to range from 8% to 20%.<sup>[14,25-27]</sup> To determine the stoichiometry of a typical large crystal, we used inductively coupled plasma mass spectroscopy (ICP-MS). Milligram-weight pieces were cut from different parts of the as-grown bulk: four pieces from the top surface of the growth and five pieces from the middle section. The latter result indicated a rather uniform bulk distribution, with an average Hg:Ba:Cu ratio of 0.88:2.08:1.06, or a Hg deficiency of about 10%. However, we found a significant inhomogeneity and Hg deficiency on the top surface of the growth, with a Hg:Ba:Cu ratio ranging from 0.75:2.02:1.22 to 0.36:2.02:1.62. This result indicates that large segments in the middle of sizable crystals, such as the one shown in Fig. 1b, are of a very good quality.

Magnetic susceptibility was measured on numerous samples and indicated a moderate sample dependence. As-grown samples are underdoped and, as shown in Fig. 2,

the mean value of  $T_c$  of a typical large as-grown sample is about 75-80 K. The transition is fairly sharp, although the small slope above 80 K indicates a gradual doping change from underdoped to optimally-doped ( $T_c$  onset of about 97 K). After annealing for five to seven days at 300-350 °C in oxygen flow, smaller crystals typically became nearly optimally-doped, with the onset  $T_c$  at 97 K and a very small transition width of  $\sim 2$  K (Fig. 2). Our annealing tests show that the optimal annealing conditions depend strongly on crystal size and shape. The  $T_c$  onset can be as high as 97 K (very close to the maximum value of  $T_c = 98$  K reported for powder samples<sup>[12]</sup>) and the transition width is typically less than 5 K for small crystals ( $\sim 10$  mg) and 8 K for large crystals. Since impurity effects tend to lower and broaden the transition,<sup>[2]</sup> this high value of  $T_c$  and the reasonably sharp transition suggest that our crystals are of the highest quality attained to date. Magnetic susceptibility measurements revealing a sharp transition in conjunction with a large superconducting volume fraction are typically interpreted in terms of a homogeneous oxygen distribution. However, this conclusion can be misleading. Preliminary resistivity measurements indicate the presence of oxygen inhomogeneities, especially in the near-surface regions. We note that annealed oxygen disorder is common to many high- $T_c$  cuprates.<sup>[2,5]</sup>

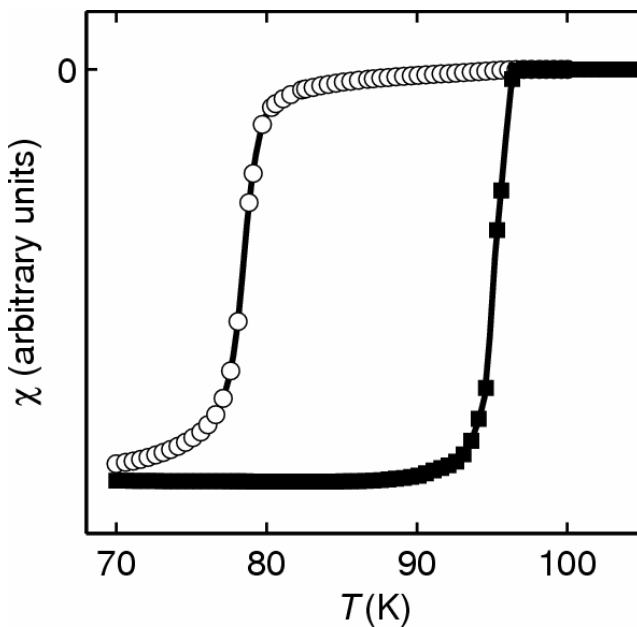


Figure 2. Magnetic susceptibility measurements of as-grown and oxygenated samples. The magnetic susceptibility for a large as-grown (open circles) and a small (6.2 mg) annealed (solid squares) sample as a function of temperature. (Susceptibility was measured with a Quantum Design MPMS-XL instrument.)

We now report on preliminary inelastic neutron scattering measurements which demonstrate that our Hg1201 crystals are suitable for detailed future studies of the structure of magnetic excitations. A central topic in the field of high- $T_c$  superconductivity has been the role of the magnetic degrees of freedom and the question if the cuprates exhibit universal magnetic excitations. Such studies require sizable single crystals. As a result, they have largely focused on single-layer  $(\text{La},\text{Sr})_2\text{CuO}_4$  ( $T_c = 38$  K at optimal doping) and two-layer  $\text{YBa}_2\text{Cu}_3\text{O}_{6+\delta}$  ( $T_c = 93$  K at optimal doping), for which such crystals have been available for some time. It has been argued that the structure of the

high-energy magnetic excitations in these two compounds is rather similar, although there also exist interesting differences at lower energies.<sup>[28-30]</sup>

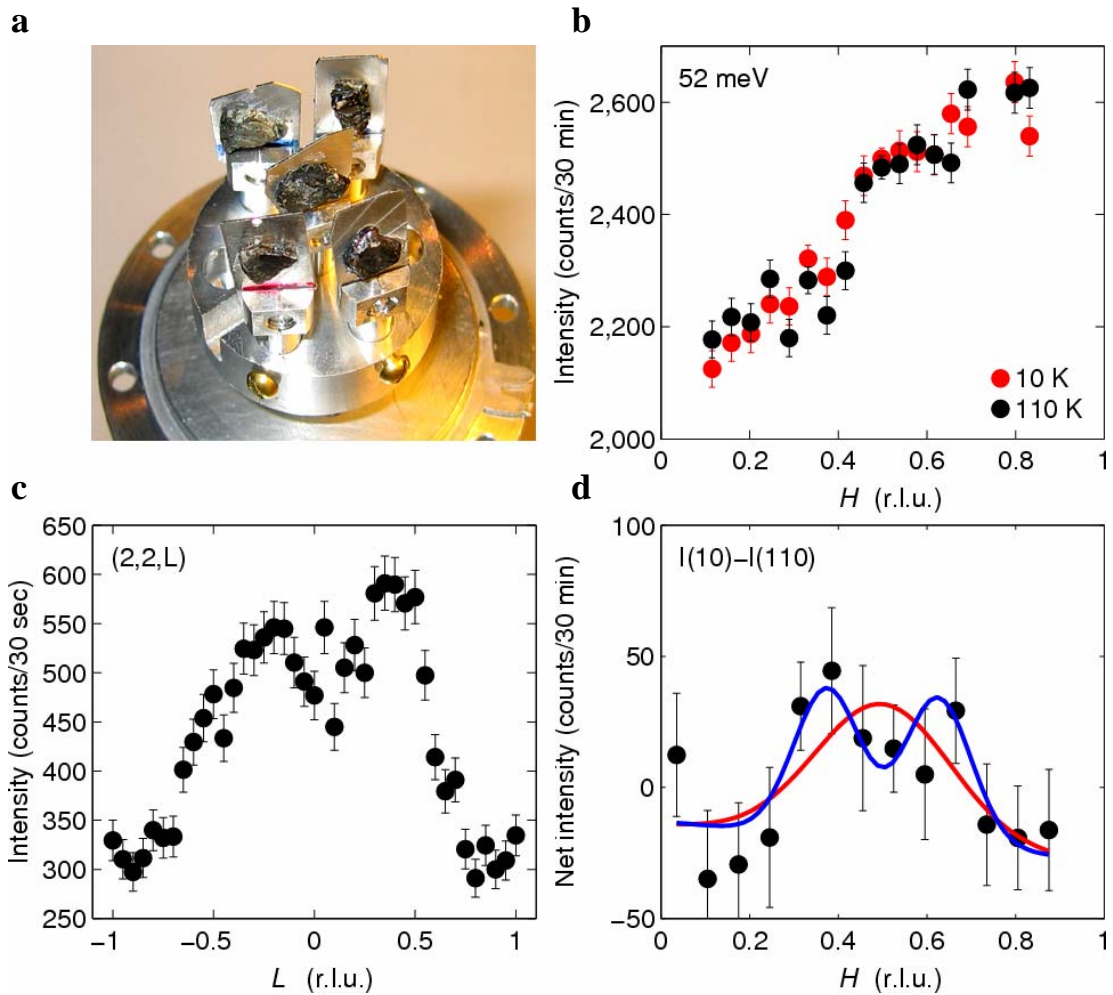


Figure 3. Hg1201 sample and inelastic neutron scattering measurements. a) Sample of five co-mounted crystals used for the inelastic neutron scattering measurements. b) Phonon characterization scan at 3 meV. c) Momentum scans (H,H,4) at an energy transfer of 52 meV at 10 K and 110 K. d) Intensity difference of the data in c), suggesting the existence of a net magnetic signal, with fits to a possible commensurate

(red) and incommensurate (blue) response. Initial crystal checks were performed at the NIST Center for Neutron Research. The inelastic experiment was performed at the 2T triple-axis spectrometer at Laboratoire Léon Brillouin, with 35 meV fixed final neutron energy and collimations set at 60-open-sample-open-open.

The neutron experiment was performed on an as-grown sample that consisted of five co-mounted crystals with total volume of  $\sim 110$  mm $^3$  mounted in the  $(H,H,L)$  zone, as shown in Fig. 3a. Based on magnetic susceptibility measurements on small crystal pieces, we estimate a superconducting transition temperature of  $T_c = 85(10)$  K for the entire sample. Bragg scattering at the  $(0,0,4)$  reflection indicated a total mosaic of  $\sim 1.5$  degrees (FWHM) for the five co-mounted crystals. In an additional characterization test, we performed a constant-energy scan along  $[2,2,L]$  at an energy transfer of 3 meV. As shown in Fig. 3b, this measurement revealed a well-defined transverse acoustic phonon branch.

To search for magnetic excitations, we performed constant- $Q$  scans at the antiferromagnetic wavevector  $Q_{\text{AF}} = (0.5, 0.5, 4)$ . Differences between scans at 10 K (superconducting state) and 110 K (normal state) indicate a maximum for an energy transfer of 52 meV (not shown). Momentum scans along  $[1,1,0]$  at that energy transfer of 52 meV, both above (110 K) and well below (10 K)  $T_c$  are shown in Fig. 3c, which reveal a relatively strong momentum dependence of the background scattering. After subtraction of the high-temperature data from those at 10 K, we found a net positive signal in the vicinity of  $Q_{\text{AF}}$ . As demonstrated in Fig. 3d, the net signal can either be described by a

single broad peak centered at  $Q_{AF}$ , or by two sharper peaks centered at incommensurate positions shifted from  $Q_{AF}$  by  $\sim 0.13$  r.l.u.

We note that the signal rate is comparable to that obtained in a study of the single-layer compound  $Tl_2Ba_2CuO_{6+\delta}$ , which investigated an optimally-doped ( $T_c \sim 90$  K) sample that consisted of  $\sim 300$  small co-mounted crystals with total volume close to that of our Hg1201 sample.<sup>[31]</sup> Recent thorough studies of  $YBa_2Cu_3O_{6+\delta}$  have revealed that the spin excitations form an hour-glass shaped dispersion centered at  $Q_{AF}$ .<sup>[32-34]</sup> At  $Q_{AF}$ , the dispersions merge into a prominent feature at  $\sim 41$  meV, the so-called  $(\pi, \pi)$  resonance, observed in the superconducting state.<sup>[33-36]</sup> The dispersions observed in  $YBa_2Cu_3O_{6+\delta}$  above and below the resonance cover a range of about 0.13.<sup>[28,32]</sup> For single-layer  $Tl_2Ba_2CuO_{6+\delta}$ , the resonance energy was found to be 47 meV. The net response at 52 meV in our slightly underdoped Hg1201 sample is consistent with these prior results, and this energy may be at or slightly above the resonance in this material.

In summary, we significantly improved the conventional encapsulation method for the growth of Hg1201 in several ways: a new vertical kettle system was employed to prepare carbon-free high-quality precursor; careful dosing of HgO is adopted to control proper vapor pressure for crystal growth; Zirconia crucibles are employed to prevent CuO creep and to facilitate the separation of crystals from the crucible. Our method results in gram-sized Hg1201 single crystals, and it can likely be extended to the double ( $n=2$ ) and triple-layer ( $n=3$ ) members of the series  $HgBa_2Ca_{n-1}Cu_nO_{2n+2+\delta}$ . The Hg1201 crystals were characterized by several experimental techniques, demonstrating their good quality. The present work provides the foundation for detailed experimental studies of this

important family of transition metal oxides, such as inelastic neutron scattering, optical spectroscopy and angle-resolved photoemission spectroscopy.

## REFERENCES

- [1] J. G. Bednorz, K. Müller, *Z. Phys. B* **1986**, *64*, 189.
- [2] H. Eisaki, N. Kaneko, D. L. Feng, A. Damascelli, P. K. Mang, K. M. Shen, Z.-X. Shen, M. Greven, *Phys. Rev. B* **2004**, *69*, 064512.
- [3] J. M. Tranquada, B. J. Sternlieb, J. D. Axe, Y. Nakamura, S. Uchida, *Nature* **1995**, *375*, 561.
- [4] C. Howald, H. Eisaki, N. Kaneko, M. Greven, A. Kapitulnik, *Phys. Rev. B* **2003**, *67*, 014533.
- [5] K. McElroy, Jinho Lee, J. A. Slezak, D.-H. Lee, H. Eisaki, S. Uchida, J. C. Davis McElroy, *Science* **2005**, *309*, 1048.
- [6] C. C. Homes, S. V. Dordevic, M. Strongin, D. A. Bonn, R. Liang, W. N. Hardy, S. Komiya, Y. Ando, G. Yu, N. Kaneko, X. Zhao, M. Greven, D. N. Basov, T. Timusk, *Nature* **2004**, *430*, 539.
- [7] L. Lu, G. Chabot-Couture, X. Zhao, J. N. Hancock, N. Kaneko, O. P. Vajk, G. Yu, S. Grenier, Y. J. Kim, D. Casa, T. Gog, M. Greven, *Phys. Rev. Lett.* **2005**, *95*, 217003.
- [8] W.S. Lee, T. Yoshida, W. Meevasana, K.M. Shen, D.H. Lu, W.L. Yang, X.J. Zhou, X. Zhao, G. Yu, Y. Cho, M. Greven, Z. Hussain, and Z.-X. Shen, *cond-mat/0606347*.
- [9] E. V. Antipov, A. M. Abakumov, S. N. Putilin, *Supercond. Sci. Technol.* **2002**, *15*, R31.
- [10] A. Wisniewski, R. Puzniak, J. Karpinski, J. Hofer, R. Szymczak, M. Baran, F.M.

Sauerzopf, R. Molinski, E.M. Kopnin, J.R. Thompson, *Phys. Rev. B* **2000**, *61*, 791.

[11] S. N. Putilin, E. V. Antipov, O. Chmaissem, M. Marezio, *Nature* **1993**, *362*, 226.

[12] A. Yamamoto, K. Minami, W.-Z. Hu, A. Miyakita, M. Izumi, S. Tajima, *Phys. Rev. B* **2002**, *65*, 104505.

[13] A. Schilling, M. Cantoni, J. D. Guo, H. R. Ott, *Nature* **1993**, *363*, 56-58.

[14] D. Pelloquin, V. Hardy, A. Maignan, B. Raveau, *Physica C* **1997**, *273*, 205.

[15] A. J. Batista-Leyva, MTD Orlando, L. Rivero, R. Cobas, E. Altshuler, *Physica C* **2003**, *383*, 365.

[16] C. T. Lin, Y. Yan, K. Peters, E. Schonherr, M. Cardona, *Physica C* **1998**, *300*, 141.

[17] A. Kareivat, I. Bryntse, *J. Mater. Chem.* **1995**, *5*, 885.

[18] K. Knizek, M. Veverka, E. Hadova, J. Hejtmanek, D. Sedmidubsky, E. Pollert, *Physica C* **1998**, *302*, 290.

[19] R. L. Meng, L. Beauvais, X. N.. Zang, Z. J. Huang, Y. Y. Sun, Y. Y. Xue, C. W. Chu, *Physica C* **1993**, *216*, 21.

[20] Y. Zhao, B. Chen, M. LaRobina, H. L. Kennedy, P. Fekitoa, *J. Mater. Sci. Lett.* **1996**, *15*, 323.

[21] V. A. Alyoshin, D. A. Mikhailova, E. V. Antipov, *Physica C* **1996**, *271*, 197.

[22] S. Lee, M. Mun, M. Bae. S. Lee, *J. Mater. Chem.* **1994**, *4*, 991.

[23] G. B. Peacock, I. Gameson, P. R. Edwards, *Adv. Mater.* **1997**, *9*, 248.

[24] P. Odier, A. Sin, P. Toulemonde, A. Bailly, S. Le Floch, *Supercond. Sci. Technol.* **2000**, *13*, 1120.

[25] J. L. Wagner, P. G. Radaelli, D. G. Hinks, J. D. Jorgensen, J. F. Mitchell, B.

Dabrowski, G. S. Knapp, M. A. Beno, *Physica C* **1993**, *210*, 447.

[26] A. Asab, A. R. Armstrong, I. Gameson, P. P. Edwards, *Physica C* **1995**, *255*, 180.

[27] V. A. Alyoshin, D. A. Mikhailova, E. B. Rudnyi, E. V. Antipov, *Physica C* **2002**, *383*, 59.

[28] J. M. Tranquada, *cond-mat/0512115*.

[29] N. B. Christensen, D. F. McMorrow, H. M. Ronnow, B. Lake, S. M. Hayden, G. Aeppli, T. G. Perring, M. Mangkorntong, M. Nohara, H. Takagi, *Phys. Rev. Lett.* **2004**, *93*, 147002.

[30] J. M. Tranquada, H. Woo, T. G. Perring, H. Goka, G. D. Gu, G. Xu, M. Fujita, K. Yamada, *Nature* **2004**, *429*, 534.

[31] H. He, P. Bourges, Y. Sidis, C. Ulrich, L. P. Regnault, S. Pailhes, N. S. Berzigerova, N. N. Kolesnikov, B. Keimer, *Science* **2002**, *295*, 1045.

[32] S. M. Hayden, H. A. Mook, P. Dai, T. G. Perring, F. Dogan, *Nature* **2004**, *429*, 531.

[33] C. Stock, W. J. L. Buyers, R. A. Cowley, P. S. Clegg, R. Coldea, C. D. Frost, R. Liang, D. Peets, D. Bonn, W. N. Hardy, R. J. Birgeneau, *Phys. Rev. B* **2005**, *71*, 024522.

[34] D. Reznik, P. Bourges, L. Pintschovius, Y. Endoh, Y. Sidis, T. Masui, S. Tajima, *Phys. Rev. Lett.* **2004**, *93*, 207003.

[35] J. Rossat-Mignod, L. P. Regnault, C. Vettier, P. Bourges, P. Burlet, J. Bossy, J. Y. Henry, G. Lapertot, *Physica C* **1991**, *185-189*, 86-92.

[36] H. A. Mook, M. Yethiraj, G. Aeppli, T. E. Mason, T. Armstrong, *Phys. Rev. Lett.* **1993**, *70*, 3490.

[37] H. F. Fong, B. Keimer, P. W. Anderson, D. Reznik, F. Dogan, I. A. Aksay, *Phys. Rev. Lett.* **1995**, *75*, 316.

[38] S. Pailhes, Y. Sidis, P. Bourges, V. Hinkov, A. Ivanov, C. Ulrich, L. P. Regnault, B. Keimer, *Phys. Rev. Lett.* **2004**, *93*, 167001.